# NLOS Multipath Detection using Convolutional Neural Network

Taro Suzuki, *Chiba Institute of Technology, Japan*
Kazuki Kusama, Yoshiharu Amano, *Waseda University, Japan*

## BIOGRAPHY (IES)

Taro Suzuki is a chief researcher at Chiba Institute of Technology, Japan. He received his BS and MS degrees and his PhD in engineering from Waseda University in 2007, 2009, and 2012, respectively. From 2012 to 2014, he worked as a postdoctoral researcher at Tokyo University of Marine Science and Technology. From 2015 to 2019, he worked as an assistant professor at Waseda University. His current research interests include GNSS precise positioning in urban environments.

Kazuki Kusama is a master's course student at Waseda University. He received his BS in mechanical engineering from Waseda University in 2018.

Yoshiharu Amano received his PhD in engineering from Waseda University in 1998, where he is a professor at the Research Institute for Science and Engineering. His research interests include sensing technologies for autonomous mobile systems and optimal design and control of power and energy systems.

## ABSTRACT

In global navigation satellite system (GNSS) positioning, GNSS satellites are often obstructed by buildings, leading to reflected and diffracted signals, which are known as non-line-of-sight (NLOS) signals. Such signals cause major GNSS positioning (also known as "NLOS multipath") errors. In this paper, a novel NLOS multipath detection technique using a machine-learning approach to improve the positioning accuracy in urban environments is proposed. The key idea behind this technique is to construct a classifier that discriminates NLOS multipath signals from the output of the multiple GNSS signal correlators of a software GNSS receiver. In the case of an NLOS signal, there are no direct signals; the first reflected signal has low power compared to a direct signal. Hence, the correlation function is expected to be more distorted in the case of an NLOS signal correlation. We use this phenomenon to detect NLOS signals. To consider the change in shape of the correlation values of NLOS signals and their temporal variation, we propose a method for constructing a convolutional neural network (CNN)-based NLOS discriminator. Furthermore, we propose a method for applying the NLOS probability, which is the output of the CNN, to the positioning calculation. To evaluate the proposed technique, we conducted NLOS classification experiments using signal correlation data acquired at different locations in the Shinjuku area of Japan. We compared the proposed method with a method using a simple NN. As the experiment results indicate, the proposed method can correctly discriminate approximately 98% of NLOS multipath signals, and the discrimination rate of the proposed CNN-based method is higher than that of the simple NN-based approach. Furthermore, we improved the positioning accuracy from 34.1 to 1.6 m using the proposed method and concluded that the proposed approach can increase the positioning accuracy in urban environments.

## INTRODUCTION

Global navigation satellite systems (GNSSs) are gaining increasing popularity owing to their wide range of current and potential applications. Significant improvements in the availability of satellite-based positioning in urban areas are expected because of an increase in the number of positioning satellites launched by various countries. Navigation signals from these satellites are expected to be used in urban contexts for applications such as intelligent transportation systems, automatic vehicle navigation, and personal navigation using smartphones. However, because of serious impacts caused by urban canyon environments on the positioning accuracy of multipath signals from positioning satellites, an increased availability of satellite positioning techniques does not necessarily equate to more precise positioning. Because multipath effects are highly dependent on the surrounding features, such as tall buildings near GNSS receivers, errors cannot be eliminated through the use of differential GNSS. Fig. 1 shows multipath signals in an urban environment. GNSS multipath signals can be divided into two types: line-

of-sight (LOS) multipath signals and non-line-of-sight (NLOS) multipath signals. In the case of LOS multipath signals, both direct and reflected/diffracted signals are simultaneously received. This affects the GNSS positioning accuracy [1]. However, various signal correlation techniques, including a narrow correlator [2] and a strobe correlator [3] can be used to mitigate LOS multipath errors [2–5]. The LOS multipath error is several meters at most. In the case of NLOS multipath signals, a GNSS receiver can receive only those multipath signals that are reflected off the surfaces of buildings or diffracted by their edges from a satellite behind the buildings. In such cases, multipath signals will have a large range of errors of several tens of meters or more in GNSS pseudorange measurements. Hence, practical techniques for NLOS signal detection are required to improve the positioning accuracy in urban environments.

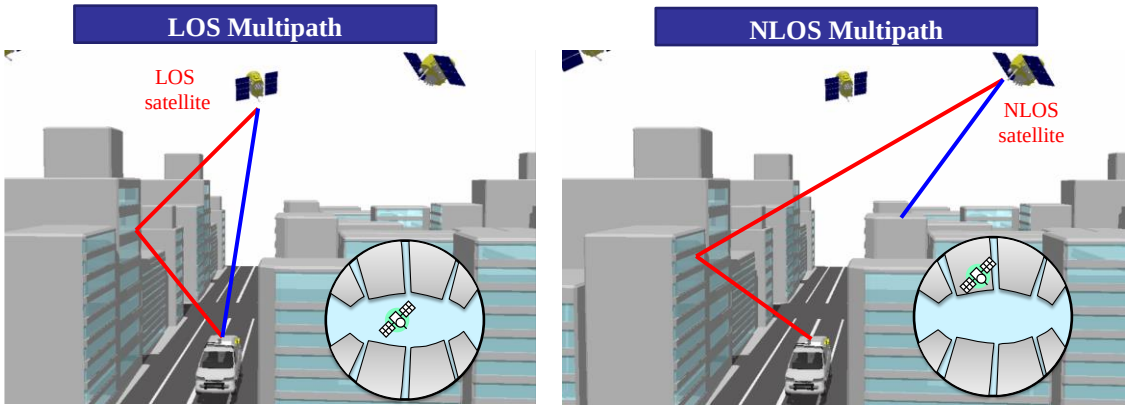

Fig. 1 LOS and NLOS multipath signals in urban environment.

NLOS signals must be identified from all received GNSS signals to mitigate NLOS multipath errors. Additional sensors are required to detect NLOS signals with GNSS receivers [6–10]. Marais et al. proposed an NLOS detection tool using an image sensor [6]. However, NLOS detection is affected by weather and illumination conditions. We previously proposed the use of a fish-eye camera and image processing technique for detecting NLOS signals [7]. This technique is more robust than the previously proposed methods, but techniques that require a visible light camera cannot be used at night. In later studies, we proposed a technique for realizing NLOS signal detection using an omnidirectional far-infrared (FIR) camera to exclude invisible satellites [8]. An omnidirectional FIR camera can easily distinguish the sky from obstacles such as buildings and can also be used at night. However, omnidirectional FIR cameras are not readily available on the market and can only be procured upon special request. The use of real-time range information from obstacles using a laser scanner to identify invisible satellites with associated NLOS multipath errors was proposed [9, 10]. However, it is difficult to apply this technique to moving vehicles to obtain their real-time position. Three-dimensional maps were also used to improve the GNSS positioning accuracy in urban environments [11–15]. However, it is difficult to directly integrate 3D map information into GNSS pseudorange-based positioning. Further, an accurate 3D model is needed to compute the position in advance. The signal-to-noise ratio (SNR) or signal strength of the received GNSS signals can typically be used to select GNSS signals that are applicable for positioning computations [16, 17]. In general, the SNRs of reflected or diffracted signals are weaker than those corresponding to the directly received signals. However, NLOS signals can occasionally be nearly as strong as directly received signals, which makes it difficult to completely mitigate NLOS multipath errors. Thus, it is difficult to identify NLOS signals from the received signals alone.

Even if NLOS discrimination can be achieved, excluding NLOS satellites from the positioning computation causes the deterioration of dilution of precision (DOP), and the number of satellites is reduced. Thus, the NLOS exclusion occasionally reduces the accuracy and availability of the positioning in an urban environment. To address this problem, correcting for NLOS multipath errors is an ideal countermeasure. A few methods for correcting NLOS multipath errors using 3D maps have been proposed [18, 19]. However, the correction of such errors is extremely complex and difficult, and remains impractical in terms of accuracy.

However, recent developments in machine learning techniques have led to a significant amount of research on improving the GNSS positioning accuracy through machine learning [20–23]. In [20], pioneering studies on the use of machine learning methods for GNSS positioning are described. We previously proposed an NLOS detection technique using a software receiver and a support vector machine (SVM) [21]. In [22], the authors proposed machine learning methods for improving the GNSS

positioning; additionally, a method for discriminating NLOS signals from the machine learning of GNSS observations, such as the SNR, is proposed. Other machine learning methods have also been increasing in number in recent years [23].

In this study, we propose a novel NLOS multipath detection technique that enhances our previously proposed method. The key idea behind this technique is to construct a classifier that discriminates the NLOS multipath signals from the set of multiple time-series GNSS signal correlator outputs. Instead of using an SVM, we use a convolutional neural network (CNN) to extract NLOS features from the correlation outputs automatically. In the case of line-of-sight (LOS) multipath signals, the direct and reflected signal correlation functions are combined. Consequently, the reflected signals distort the code correlation function of the direct signal. In the case of an NLOS signal, there are no direct signals; the combined correlation function is more distorted than in the case of LOS multipath signals. We use this phenomenon to detect NLOS signals by applying a CNN. Further, we propose a positioning method that applies the probability of the NLOS signal, which is the output of the proposed CNN, to the positioning computation.

The contributions of this study are as follows:

1. Direct machine learning of a GNSS signal correlation output, which is the most primitive GNSS signal processing output, is an innovative approach. There have been no examples of applying a CNN to detect NLOS signals in multiple GNSS constellations, and NLOS discrimination using a CNN has been a significant achievement.

2. We propose a new method for using the NLOS probability determined by a CNN in actual GNSS positioning. Instead of excluding NLOS satellites, we add weights based on the NLOS probability to GNSS pseudorange observations to improve the accuracy and availability of GNSS positioning in urban environments.

3. We applied the proposed machine learning method to GNSS signals acquired in a real urban environment and showed that the positioning accuracy is improved using actual GNSS positioning in such an environment.

The remainder of this paper is organized as follows. First, we describe the details of the proposed method and its basic principles for detecting an NLOS. We then describe an NLOS multipath detection algorithm using a CNN and its network configuration. Next, we extend the proposed NLOS detection algorithm to a multi-GNSS constellation. Furthermore, we present a positioning method using NLOS probabilities. We then describe the evaluation of NLOS multipath detection in an actual environment, and provide the positioning results. Finally, we present some concluding remarks regarding this research.

## NLOS CORRELATION FUNCTION

A feature of the proposed method is that it discriminates the NLOS signal by directly learning the correlation output of the NLOS multipath signal; the correlation function of the NLOS multipath signal is significantly distorted compared to the LOS multipath signal with a direct signal. First, the shape of the correlation function for the LOS and NLOS multipath signals is clarified. The GNSS direct signal $S_0(t)$ can be expressed as follows:

$$S_0(t) = A_0 \cdot C(t - \tau_0) \cdot \cos(\omega t + \theta_0), \tag{1}$$

where $C(t)$ denotes the GNSS-spreading code sequence, and $A_0$, $\omega_0$, $\tau_0$, and $\theta_0$ are the amplitude, signal code delay of a direct signal, and carrier phase, respectively. In addition, $\omega_0$ is the angular frequency of the GNSS signal. To simplify the problem, we consider the case in which the direct signal $S_0(t)$ is affected by the single delayed reflected signal $S_1(t)$. The LOS multipath signal $S_{\mathrm{LOS}}(t)$ can be expressed as follows:

$$\begin{aligned} S_{\mathrm{LOS}}(t) &= S_0(t) + S_1(t) \\ &= S_0(t) + A_1 \cdot C(t - \tau_0 - \tau_1) \cdot \cos(\omega t + \theta_0 + \Delta\phi_1)' \end{aligned} \tag{2}$$

where $A_1$, $\tau_1$, and $\Delta\phi_1$ are the multipath amplitude, delay, and relative phase between direct and multipath signals, respectively. The correlation function of the direct signal is distorted by these three multipath parameters. Fig. 2(a) illustrates the signal correlation functions of the LOS multipath signal. Here, the multipath amplitude ratio $\alpha_{\mathrm{LOS}} = A_0/A_1$ is 0.5, the multipath delay $\tau_1$ is 0.5 chips, and the relative phase $\Delta\phi_1$ is $0^\circ$ (in-phase). Here, the multipath amplitude ratio $\alpha_{\mathrm{LOS}}$ is a major factor distorting the correlation function of the LOS multipath signal. The smaller the amplitude of the reflection or diffraction signal with respect to the direct signal, the smaller the effect is on the correlation function of the direct signal. In general, the first reflected

signal has low power compared to a direct signal. The reflection and diffraction signals have a smaller amplitude than direct signals because they lose energy during reflection and diffraction. As a result, the shape of the correlated output of the LOS multipath signal with a direct signal becomes a clean triangular shape with only a single peak.

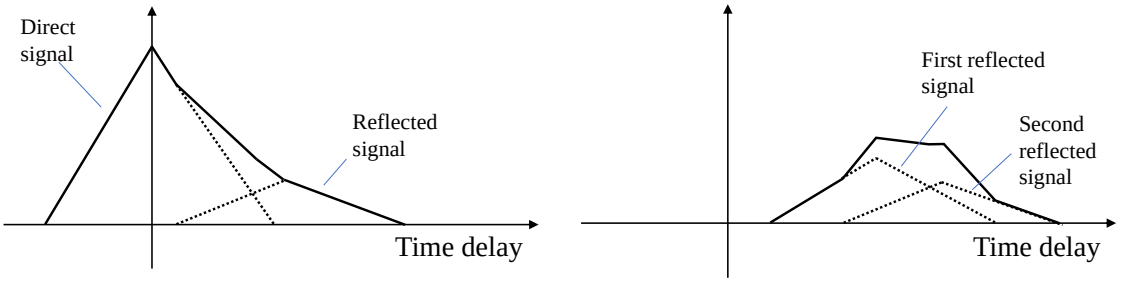


(a) LOS multipath correlation function (b) NLOS multipath correlation function

Fig. 2 LOS and NLOS multipath correlation functions. The NLOS multipath correlation function is more distorted than the LOS multipath correlation function.

In the case of the NLOS correlation function, there is no direct signal, and the first reflected signal is distorted by the second reflected signal. Fig. 2(b) shows the NLOS signal correlation function of the NLOS multipath signal. The NLOS multipath signal can be expressed as follows:

$$\begin{aligned} S_{\mathrm{NLOS}}(t) &= S_1(t) + S_2(t) \\ &= S_1(t) + A_2 \cdot C(t - \tau_1 - \tau_2) \cdot \cos(\omega t + \theta_1 + \Delta\phi_2)' \end{aligned} \tag{3}$$

The NLOS signal correlation function is a combination of the reflected and diffracted signal correlations. In the case of NLOS signals without a direct signal, the amplitude ratio between the first and second signals is not considered to be much different. Therefore, the amplitude ratio $\alpha_{\mathrm{NLOS}}$ is close to 1. The amplitude ratio between the LOS multipath $\alpha_{\mathrm{LOS}}$ and NLOS multipath $\alpha_{\mathrm{NLOS}}$ has the following relationship:

$$\alpha_{\mathrm{LOS}} < \alpha_{\mathrm{NLOS}}. \tag{4}$$

Therefore, the NLOS correlation function is more susceptible to the second signal than the LOS correlation function, resulting in a large distortion of the correlation function. For this reason, the NLOS correlation function does not have an ideal, clean triangular shape. We also consider the effect of the relative phase on the correlation function. From Equations (2) and (3), the shape of the signal correlation function depends on the phase of the second signal relative to the first signal. If the relative phase is 90°, the second signal has no effect on the correlation function of the first signal. When the antenna is stationary, the phase of the reflected signal relative to the direct signal generally changes slowly as the satellite moves. The NLOS signal, on the other hand, has a large relative phase variation owing to the complex synthesis of multiple reflections and diffraction signals. As a result, the correlation function of the NLOS signal is expected to become unstable over time. We use these phenomena to detect NLOS signals. We created an NLOS classifier based on the machine learning of the NLOS correlation shape.

## OVERVIEW OF THE PROPOSED METHOD

To discriminate the NLOS signal from the shape of the correlation values, we use a CNN in this study. By using a CNN, it is possible to extract features related not only to the shape of the correlation function but also to the time-dependent NLOS features. Fig. 3 shows the concept of the proposed method. Fig. 3(a) illustrates the time-series correlator outputs of the LOS signal. The right side of Fig. 3(a) shows a 2D image of the time-series correlator outputs. Fig. 3(b) shows the same correlator outputs in the NLOS signals. In the 2D image on the right side of Fig. 3, the closer the color is to red, the higher the normalized correlation. Compared with the LOS signal (Fig. 3(a)), the shape of the NLOS correlation is distorted and becomes unstable over time. The CNN can learn these NLOS features from the 2D correlation image. The proposed method does not require additional sensors and is practicable and easy to implement.

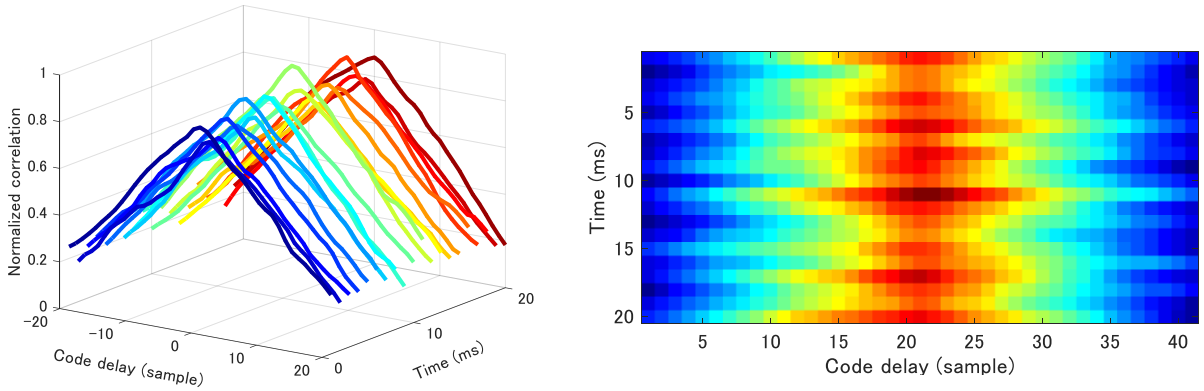


(a) Correlation outputs and correlation image in LOS signals

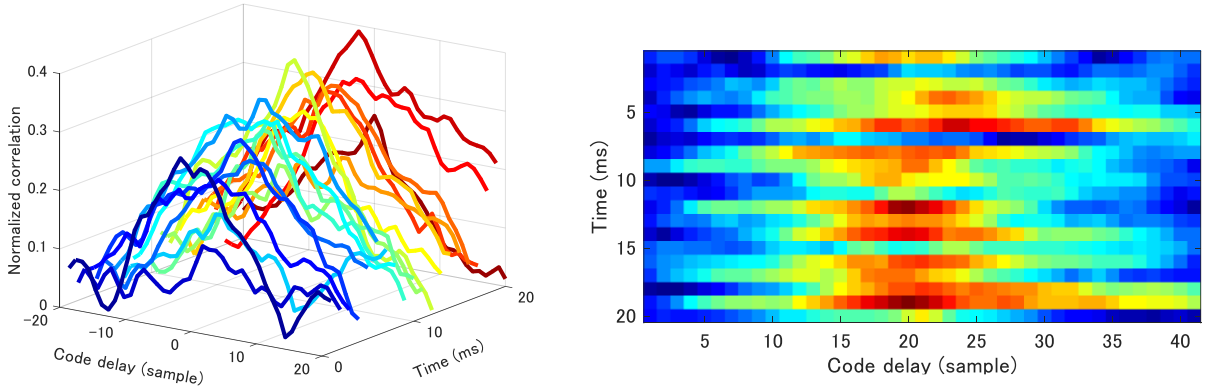


(b) Correlation outputs and correlation image in NLOS signals.

Fig. 3 Concept of proposed NLOS classification system. We use a CNN to learn the NLOS features in GNSS signal correlation outputs.

## PROPOSED CNN ARCHITECTURE

The proposed method uses the shape and time variation of the GNSS signal correlation outputs to determine the NLOS signals. Fig. 4 shows an overview of the proposed NLOS classification system and network architecture. We use two convolutional layers (before the pooling layer) to extract NLOS features from the raw correlation input with two dimensions. First, we generate a 2D correlation image for each satellite from raw correlator outputs. To compute the GNSS signal correlation, we use a software GNSS receiver. The correlation shape is dependent on the sampling frequency of the incoming signals. In this study, we used a sampling frequency of 26 MHz; thus, the number of correlation points within the +-1 code chip is 26 × 2 + 1 = 53 points. However, owing to the computational processing time, we used 27 correlation points for the input of the CNN. We store every 1 ms correlation output for 20 ms, and then generate a 27 × 20 input image. The first convolutional layer filters the 27 × 20 input image with 32 kernels of 3 × 3 in size with a stride of 1 pixel. A global max-pooling is then applied to the filter. The second convolutional layer takes as input the max-pooled output of the first convolutional layer and filters it with 64 kernels 2 × 2 in size. Max-pooling is then applied to the filter. In these convolutional filters, the activation function is applied to the output of the filters. In this study, the rectified linear unit (ReLU) function is used for the convolution output. Finally, fully connected layers are followed by a softmax classifier. The global features are fed to the softmax classifier to determine the probability of LOS and NLOS signals.

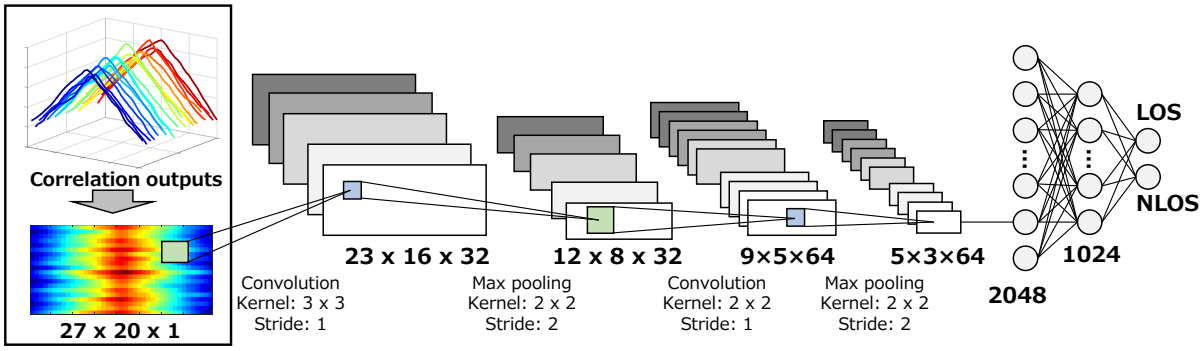


Fig. 4 Overview of the proposed NLOS classification system using a CNN.

A CNN requires a large volume of training datasets for learning. We collected the actual NLOS correlation outputs using a software GNSS receiver installed in an urban environment. The problem here is obtaining the correct reference of LOS/NLOS signals from all received signals. We need to use additional sensors to determine the NLOS signals for training because it is difficult to determine reliable NLOS signals using signals alone. In this study, we use a fish-eye camera and manually check the NLOS signals from the captured image. Satellite positions computed from a GNSS ephemeris are projected onto the fish-eye image, and the NLOS signals are easily determined manually. We conducted a fish-eye camera calibration in advance to correctly project the satellite position onto the fish-eye image. Note that an accurate orientation angle of the camera is needed to determine the NLOS signals from the fish-eye image. In this study, we determined the camera orientation from the information of the azimuth angle of the buildings and other objects captured in the image. We generate a virtual fish-eye image using the 3D city model and its approximate position. We estimate the orientation angle of the camera to match the captured image and the virtual fish-eye image generated from the 3D city model. The NLOS signals, thus determined, are used as training data for the CNN.

We describe the pre-processing of the input data for the proposed CNN. The output correlation value from a software receiver is normalized based on the elevation angle of the satellite. The magnitude of the correlation value is related to the GNSS signal strength. In general, the signal strength of the reflected or diffracted signals is weaker than that of the directly received signals. As a result, the signal strength can be used to detect NLOS signals. Even in ordinary GNSS positioning calculations, the SNR, which represents the GNSS signal strength, is widely used to exclude an NLOS multipath signal and to select satellites for positioning calculations. Because the signal strength of the GNSS is considered to be a good representation of the NLOS signal, both the shape of the signal correlation shape and the magnitude of the signal correlation value should be used for NLOS discrimination. However, the signal strength is also dependent on the satellite elevation angle. We model the maximum correlation values in an open-sky environment using the actual observed data to normalize the correlation outputs. The polynomial function that represents the relationship between the satellite elevation and the maximum correlation value is determined through regression from the actual data obtained in an open-sky environment. Here, we express the open-sky maximum correlation value $\eta(\theta_{el})$ as a fourth-order polynomial at an elevation angle with an approximate maximum correlation value as the coefficient.

$$\eta(\theta_{el}) = a_4\theta_{el}^4 + a_3\theta_{el}^3 + a_2\theta_{el}^2 + a_1\theta_{el} + a_0. \quad (5)$$

The coefficients $a_0$ through $a_4$ are then estimated using the least-squares method. We normalize the signal correlation by dividing the maximum signal correlation by $\eta(\theta_{el})$, and include in the CNN a feature in which the NLOS signal has a lower strength than the LOS signal. Finally, the pre-processed input data are converted into a 2D image, and the NLOS discriminator is acquired by the learning of a CNN.

## NLOS CLASSIFICATION FOR MULTI-GNSS SIGNALS

In our previous study [21], an SVM-based classification of the GPS LOS/NLOS signals using a software receiver was proposed, and it was shown that the positioning accuracy was improved to exclude the identified NLOS signals. However, by extending the proposed method to GNSS such as GLONASS, BeiDou, and Galileo, the number of GNSS satellites in urban environments will increase, and it is expected to improve the positioning accuracy in dense urban environments where the position computation is difficult to achieve using only GPS. However, the shape of the signal correlation value differs from that of GPS

because each satellite system has a different signal structure (chip rate, code length, and modulation scheme). In addition, because the frequency of the signal is different, the peak of the signal correlation value from a satellite at the same elevation angle is considered to differ depending on the antenna used.

To cope with these problems, we use a CNN to train an individual discriminator for each satellite signal. The target signals applied in this paper are GPS L1C/A, GLONASS G1, Galileo E1, and BeiDou B1 signals. The details of each signal and its parameters in the network structure of the CNN are shown in Table 1. Among these signals, Galileo's E1 signal is significantly different from that of the other signals. Because the E1 signal employs a composite binary offset carrier (CBOC) modulation, it is very different from other signals whose correlation function is a BPSK signal and has multiple peaks. However, the correlation shape of the NLOS signal is distorted compared to the LOS correlation waveform as well as the L1C/A signal. Therefore, the NLOS discriminator of the CBOC signals is trained in the same way using the CNN network configuration described in the previous section. In addition, the normalization of the correlation value input described in the previous section was also compensated for each signal by applying the elevation angle and the correlation value from the measured values. A regression model was created and normalized for each satellite signal. Fig. 5 shows the actual signal correlation shape of each received satellite signal. Here, the sampling rate $f_s$ of the software receiver is commonly $f_s$ = 26 MHz. To make the input to the CNN common, we use the following approach for each satellite signal to preprocess the input data to the CNN.

**GLONASS G1:**
The code rate is 0.511 Mcps, which is half that of GPS L1C/A. Therefore, the number of correlation points in one chip is twice that in the L1C/A code. To match the number of correlation points in one chip, we used a correlation space of $4/f_s$. The input data will be 27 × 20 images.

**Galileo E1:**
The code rate is equivalent to the GPSL1C/A signal, but the code length is 4092, which is four-times as long as the L1C/A code. Therefore, the period of one code is 4 ms. To match the dimensions in the time direction, the E1 code is divided into four parts, and the correlation value per millisecond is computed. As a result, a 27 × 20 image size is generated. The Galileo E1 signal uses CBOC modulation; thus, the correlation function has multiple peaks. However, we directly use the shape of the CBOC function for NLOS classification.

**BeiDou B1:**
Because the code rate is 2.046 Mcps, which is twice as high as that of the other signals, the number of correlation points in one chip length is half that of the L1CA code. Therefore, to match the number of correlation points with the GPS L1 C/A code, we use a correlation space of $1/f_s$. Here, the correlation space of GPS L1C/A is $2/f_s$.

As described above, the NLOS discriminator is trained for each signal of each satellite system, and the NLOS discriminator learned independently for each signal is applied when NLOS discrimination is used.

Table 1 Signal specifications and CNN parameters

| | GPS L1C/A | GLONASS G1 | Galileo E1 | BeiDou B1 |
|---|---|---|---|---|
| Code rate | 1.023 Mcps | 0.511 Mcps | 1.023 Mcps | 2.046 Mcps |
| Code length | 1023 | 511 | 4092 | 2046 |
| Code period | 1 ms | 1 ms | 4 ms (Split into 1 ms) | 1 ms |
| Modulation | BPSK | BPSK | CBOC | BPSK |
| Correlation space | $2/f_s$ | $4/f_s$ | $2/f_s$ | $1/f_s$ |
| Input of CNN | 27 × 20 correlation points | | | |

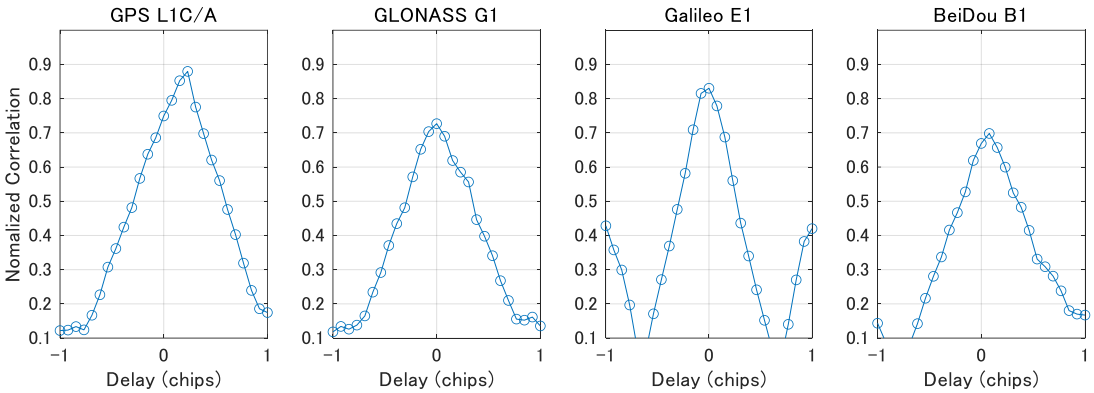

Fig. 5 Normalized correlation outputs of LOS signal. We use GPS L1C/A, GLONASS G1, Galileo E1, and BeiDou B1 signals for constructing the NLOS classifier using a CNN.

## WEIGHTING OF GNSS OBSERVATIONS BASED ON CLASSIFICATION RESULTS

Using the method described in the previous section, we discriminate whether the received signal is a LOS or an NLOS signal from the GNSS signal correlation output. By excluding the identified NLOS signals from the positioning, it is possible to improve the positioning accuracy and availability. In this paper, we propose a positioning method using NLOS probabilities estimated by the NLOS discriminator. It is difficult to determine the probability of each classification class in the SVM classification proposed in previous studies. By contrast, CNN classification can represent the classification probability of each class by applying the softmax layer, as described above. In a simple LOS/NLOS binary classification, a 50% probability can be used as a threshold. However, there are various patterns of satellite shielding in the reception of a GNSS by actual urban environments. For example, there are many signals, including degraded LOS signals caused by trees and signals from satellites near the edges of a building, that are difficult to identify clearly as NLOS signals. Based on the results of these LOS/NLOS and simple LOS/NLOS binary classifications, the rejection of NLOS signals can lead to a deterioration of the DOP and a decrease in the number of satellites used for positioning in an urban environment. As a result, although the NLOS signal is eliminated, the positioning accuracy may deteriorate, or the positioning solution may not be computed.

Therefore, in this paper, we propose a method for weighting pseudo-range observations of a GNSS using the probability of an NLOS as estimated using a CNN. Assuming that the NLOS classification probability represents the quality of the GNSS signal, we propose a method for computing a positioning solution using the weighted least-squares method by adding weights corresponding to the NLOS classification probabilities to the observed values. The pseudo-range observation equation is expressed as follows:

$$\Delta\rho = H\Delta x + \epsilon, \tag{6}$$

where $H$ is the design matrix of the unit vectors pointing from the linearization point to the location of the satellite, and $\Delta x$ is the vector offset of the user's true position and time bias from the values at the linearization point. The weighted least squares method is expressed in the following equation [25]:

$$\Delta x = (H^T W H)^{-1} H^T W \Delta\rho, \tag{7}$$

where $W$ is the weighting matrix, in which the diagonal elements are made up of the inverse of the variance of the pseudorange measurement errors. In general, the weighting matrix is designed based on the SNR or elevation angle of the satellites. However, these commonly used weight matrices cannot properly handle the weights for NLOS signals. We design the weighting matrix from the estimated NLOS classification probability. The pseudo-range from the NLOS satellite does not contain the correct distance information and should not be used for positioning. Therefore, to reduce the weights when the NLOS probability $p_{\mathrm{NLOS}}$ is high, we design the variance of the pseudo-ranges as follows:

$$\sigma^2 = \beta + \exp\left(\frac{1}{(1-p_{NLOS})}\right), \tag{8}$$

where $\beta$ is a constant parameter of the model. Using Eq. (8), as the NLOS probability approaches 100%, the weights become extremely minimal. The proposed method of dynamically adjusting the least-squares weights based on the NLOS probability makes it possible to use more satellite observations in urban environments for positioning than the method of simply dismissing NLOS signals, which is expected to improve the positioning accuracy.

## NLOS CLASSIFICATION TEST

We evaluated the NLOS classification performance of the proposed method. NLOS classification experiments were conducted using signal correlation data acquired at different locations in the Shinjuku area of Japan. Fig. 6 shows the experimental environment and the captured sky image at each location. In this environment, as shown in Fig. 6, there are many high-rise buildings of over 100 m, and NLOS multipath signals frequently occur. The training data were collected at five locations shown in Fig. 6 using the GNSS software receiver [24]. We used the NLOS training data acquisition devices to acquire three sets of 5-min signal correlation data at different times. Because the location of the satellites varies significantly over time, we obtain a variety of GNSS LOS and NLOS signal correlation outputs and use them for training. The acquired signal correlation outputs are labeled as LOS/NLOS, and we trained the discriminator. We evaluated the classification performance using the cross-validation method. We repeat the process of using 4 out of 5 data points for training and the remaining 1 data point for evaluation of the mean classification rate. We use a normal NN (without using a convolution) to compare the proposed CNN.

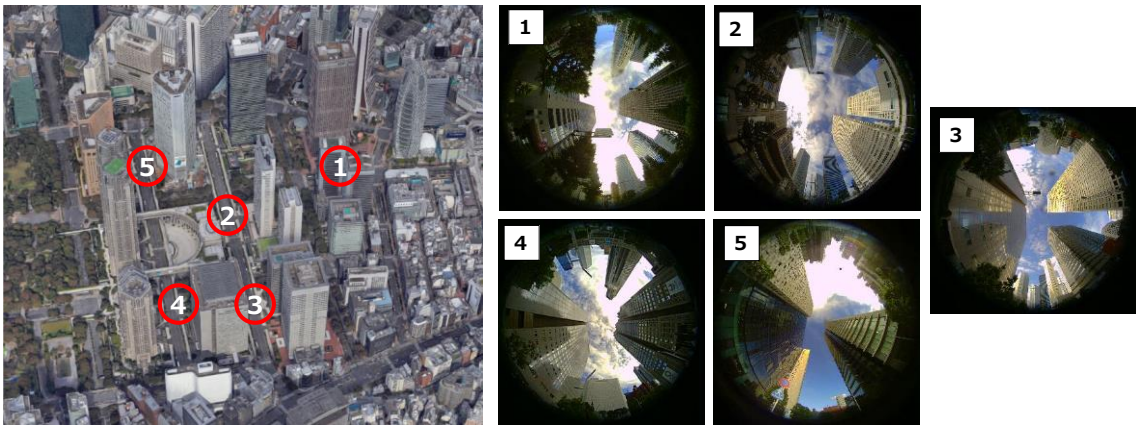

Fig. 6 Experimental environments (Shinjuku area in Japan).

We employ MATLAB to construct the NLOS signal classifier using a CNN. The parameters set for machine learning are listed in Table 2. The normalized correlation output was used as an input to the NN and CNN, and 20 ms correlation outputs were used for training. These hyperparameters were determined empirically through trial and error.

Table 2 Parameters for NN and CNN.

| | NN | CNN |
|---|---|---|
| Input | Normalized correlation outputs Size: 510 × 1 | Normalized correlation outputs Size: 27 × 20 |
| Output | Two classes (LOS/NLOS) with probability | |
| Batch size | 1024 | |
| Learning rate | 0.01 | |
| Optimizer | Adam | |

Tables 3 and 4 show the results of the LOS and NLOS classification using the proposed method. It can be confirmed that the proposed CNN has the best classification performance compared with the other methods. The classification rate at which a signal from the NLOS signal group was correctly classified as an NLOS signal was 97.9% when using the proposed method.

The classification rate of the LOS signal increased from 97.1% to 98.3% compared with the use of the conventional neural network.

Table 3 LOS classification performance of the proposed method

| | Test #1 | Test #2 | Test #3 | Test #4 | Average |
|---|---|---|---|---|---|
| NN | 97.2 % | 98.7 % | 98.6 % | 93.9 % | 97.1 % |
| CNN | 99.0 % | 97.8 % | 99.7 % | 96.7 % | 98.3 % |

Table 4 NLOS classification performance of the proposed method

| | Test #1 | Test #2 | Test #3 | Test #4 | Average |
|---|---|---|---|---|---|
| NN | 88.8 % | 96.1 % | 99.1 % | 99.9 % | 96.0 % |
| CNN | 94.5 % | 98.0 % | 99.2 % | 99.9 % | 97.9 % |

## POSITIONING TEST USING THE PROPOSED METHOD

Positioning tests were conducted in the Shinjuku area, which is a different location from that where the training data were acquired. Fig. 7 shows the sky image of the test environment, with the actual received GNSS signals projected onto the fish-eye image.
Table 5 lists the results of the classification achieved using the proposed method. From Fig. 11 and Table 5, it can be seen that many satellites are correctly classified.

We used RTKLIB [26], which is a GNSS positioning tool developed as an open-source software, to calculate the antenna position. Fig. 8 shows a comparison of the positioning results when using the proposed method. The blue points in Fig. 8 indicate the single-point positioning results without applying the proposed method. Note that we use the SNR mask (35 dB-Hz) and satellite elevation mask (15°) to exclude NLOS signals. However, a large positioning error remains in the NLOS environment. By contrast, if we use the proposed method, the positioning error is dramatically decreased (red points in Fig. 8). By weighting the LOS satellite, a large positioning error can be removed, and the horizontal root mean square error is reduced from 34.1 to 1.6 m.

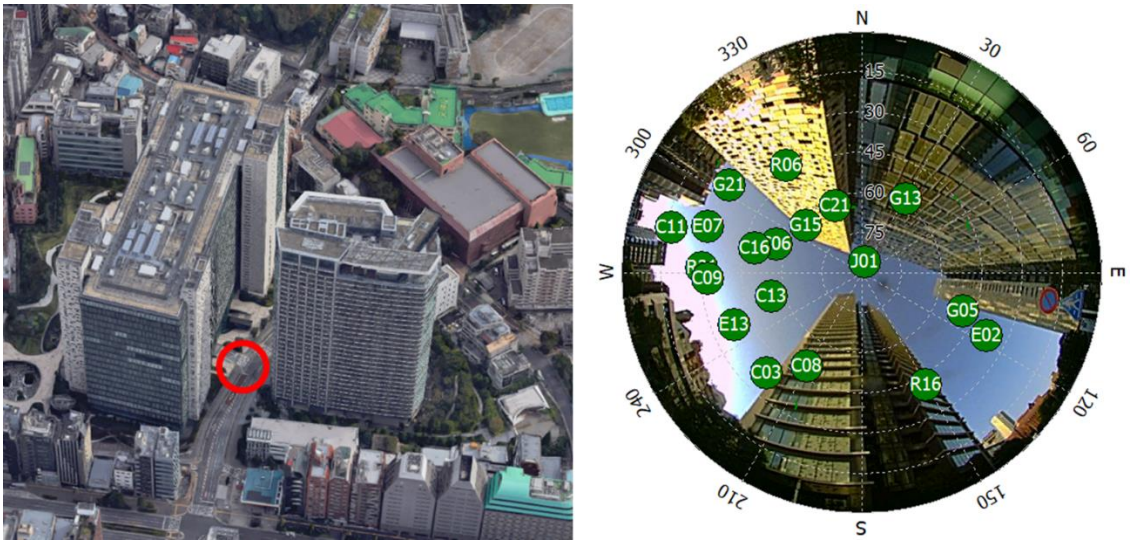

Fig. 7 Experimental environment and satellite constellation for static positioning experiment.

Table 5 NLOS classification results. L denotes a LOS satellite, and N denotes an NLOS satellite.

| Satellite | G05 | G13 | G15 | G21 | E02 | E07 | J01 | R06 | R16 |
|---|---|---|---|---|---|---|---|---|---|
| LOS/NLOS reference | L | N | N | L | L | L | L | N | N |
| NLOS probability | 0.6 % | 96.7 % | 100 % | 21.0 % | 0.1 % | 0.0 % | 0.0 % | 96.6 % | 99.9 % |
| Satellite | R21 | C03 | C06 | C08 | C09 | C11 | C13 | C16 | C21 |
| LOS/NLOS | L | L | L | N | L | L | L | L | N |
| NLOS probability | 0.0 % | 13.0 % | 7.3 % | 99.9 % | 0.0 % | 2.2 % | 12.1 % | 0.4 % | 100 % |

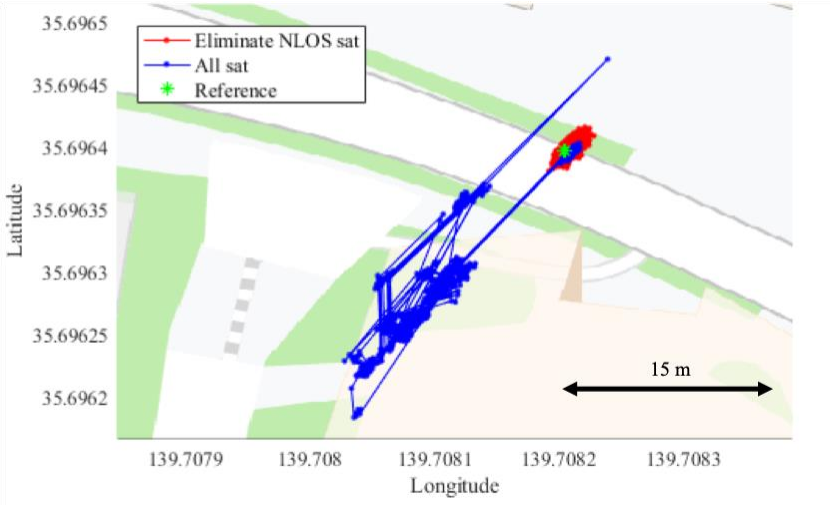


Fig. 8 Positioning results of static positioning experiment.

## CONCLUSION

In this study, we developed a method for distinguishing between LOS and NLOS signals from the signal correlation outputs using a CNN to improve the positioning accuracy in urban environments. We proposed a CNN architecture to determine the NLOS signals. Using the CNN, the NLOS feature related to the shape and time variation of the GNSS signal correlation outputs is automatically extracted and used for classification. From the classification test using actual GNSS data collected in an urban environment, the proposed method can correctly discriminate approximately 98% of the NLOS multipath signals. Further, we proposed a method for estimating the user position by weighting the GNSS observations based on the LOS/NLOS probabilities, which are output from a CNN. We can improve the positioning accuracy from 34.1 to 1.6 m using the proposed method, and we determined that the proposed method can improve the positioning accuracy in an urban environment.

## REFERENCES


1. P. D. Groves, Z. Jiang, M. Rudi, and P. Strode, "A portfolio approach to NLOS and multipath mitigation in dense urban areas," in Proc. of ION GNSS+ 2013, Institute of Navigation, 2013, vol. 4, pp. 3231–3247.
2. A. J. Van Dierendonck, P. Fenton, and T. Ford, "Theory and Performance of Narrow Correlator Spacing in a GPS Receiver," Navig. J. Inst. Navig., vol. 39, no. 3, pp. 265–283, 1992, doi: 10.1002/j.2161-4296.1992.tb02276.x.
3. L. Garin, F. van Diggelen, and J. M. Rousseau, "Strobe & Edge Correlator multipath mitigation for code," in Proc. of ION GPS 1996, Institute of Navigation, 1996, vol. 1, pp. 657–664.
4. M. S. Braasch, "Performance comparison of multipath mitigating receiver architectures," in Proc. of IEEE Aerospace Conference, 2001, vol. 3, pp. 31309–31315, doi: 10.1109/aero.2001.931361.

5. J. M. Tranquilla, J. P. Carr, and H. M. Al-Rizzo, "Analysis of a Choke Ring Groundplane for Multipath Control in Global Positioning System (GPS) Applications," IEEE Trans. Antennas Propag., vol. 42, no. 7, pp. 905–911, 1994, doi: 10.1109/8.299591.
6. J. Marais, M. Berbineau, and M. Heddebaut, "Land mobile GNSS availability and multipath evaluation tool," IEEE Trans. Veh. Technol., vol. 54, no. 5, pp. 1697–1704, Sep. 2005, doi: 10.1109/TVT.2005.853461.
7. T. Suzuki and N. Kubo, "N-LOS GNSS signal detection using fish-eye camera for vehicle navigation in urban environments," in Proc. of ION GNSS+ 2014, Institute of Navigation, 2014, vol. 3, pp. 1897–1906.
8. T. Suzuki, M. Kitamura, Y. Amano, and T. Hashizume, "Multipath mitigation using omnidirectional infrared camera for tightly coupled GPS/INS integration in urban environments," in Proc. of ION GNSS 2011, Institute of Navigation, 2011, vol. 4, pp. 2914–2922.
9. D. Maier and A. Kleiner, "Improved GPS sensor model for mobile robots in urban terrain," in Proc. of IEEE International Conference on Robotics and Automation, 2010, pp. 4385–4390, doi: 10.1109/ROBOT.2010.5509895.
10. W. Wen, G. Zhang, and L. T. Hsu, "Exclusion of GNSS NLOS receptions caused by dynamic objects in heavy traffic urban scenarios using real-time 3D point cloud: An approach without 3D maps," in 2018 IEEE/ION Position, Location and Navigation Symposium, PLANS 2018 - Proceedings, 2018, pp. 158–165, doi: 10.1109/PLANS.2018.8373377.
11. P. D. Groves, "Shadow matching: A new GNSS positioning technique for urban canyons," J. Navig., vol. 64, no. 3, pp. 417–430, Jul. 2011, doi: 10.1017/S0373463311000087.
12. R. Kumar and M. G. Petovello, "A novel GNSS positioning technique for improved accuracy in Urban canyon scenarios using 3D city model," in 27th International Technical Meeting of the Satellite Division of the Institute of Navigation, ION GNSS 2014, 2014, vol. 3, pp. 2139–2148.
13. L. T. Hsu, Y. Gu, and S. Kamijo, "3D building model-based pedestrian positioning method using GPS/GLONASS/QZSS and its reliability calculation," GPS Solut., vol. 20, no. 3, pp. 413–428, Jul. 2016, doi: 10.1007/s10291-015-0451-7.
14. T. Suzuki, "Integration of GNSS positioning and 3D map using particle filter," in Proc. of ION GNSS+ 2016, Institute of Navigation, 2016, vol. 2, pp. 1296–1304, doi: 10.33012/2016.14857.
15. P. D. Groves and M. Adjrad, "Likelihood-based GNSS positioning using LOS/NLOS predictions from 3D mapping and pseudoranges," GPS Solut., vol. 21, no. 4, pp. 1805–1816, Oct. 2017, doi: 10.1007/s10291-017-0654-1.
16. H. Tokura, H. Yamada, N. Kubo, and S. Pullen, "Using Multiple GNSS Constellations with Strict Quality Constraints for More Accurate Positioning in Urban Environments," Positioning, vol. 05, no. 04, pp. 85–96, 2014, doi: 10.4236/pos.2014.54011.
17. P. D. Groves and Z. Jiang, "Height aiding, C/N0 weighting and consistency checking for gnss nlos and multipath mitigation in urban areas," J. Navig., vol. 66, no. 5, pp. 653–669, Sep. 2013, doi: 10.1017/S0373463313000350.
18. W. Wen, G. Zhang, and L. T. Hsu, "Correcting NLOS by 3D LiDAR and building height to improve GNSS single point positioning," Navig. J. Inst. Navig., vol. 66, no. 4, pp. 705–718, Dec. 2019, doi: 10.1002/navi.335.
19. T. Suzuki and N. Kubo, "Correcting GNSS multipath errors using a 3D surface model and particle filter," in Proc. of ION GNSS+ 2013, Institute of Navigation, 2013, vol. 2, pp. 1583–1595.
20. R. Yozevitch, B. Ben Moshe, and A. Weissman, "A Robust GNSS LOS/NLOS Signal Classifier," Navig. J. Inst. Navig., vol. 63, no. 4, pp. 429–442, Dec. 2016, doi: 10.1002/navi.166.
21. T. Suzuki, Y. Nakano, and Y. Aman, "NLOS multipath detection by using machine learning in urban environments," in 30th International Technical Meeting of the Satellite Division of the Institute of Navigation, ION GNSS 2017, 2017, vol. 6, pp. 3958–3967, doi: 10.33012/2017.15291.
22. B. Xu, Q. Jia, Y. Luo, and L. T. Hsu, "Intelligent GPS L1 LOS/multipath/NLOS classifiers based on correlator-, RINEX- and NMEA-level measurements," Remote Sens., vol. 11, no. 16, p. 1851, Aug. 2019, doi: 10.3390/rs11161851.
23. Q. Liu, Z. Huang, and J. Wang, "Indoor non-line-of-sight and multipath detection using deep learning approach," GPS Solut., vol. 23, no. 3, Jul. 2019, doi: 10.1007/s10291-019-0869-4.
24. T. Suzuki and N. Kubo, "GNSS-SDRLIB: An open-source and real-time GNSS software defined radio library," in 27th International Technical Meeting of the Satellite Division of the Institute of Navigation, ION GNSS 2014, 2014, vol. 2, pp. 1364–1375.
25. E. Kaplan and C. Hegarty, Understanding GPS: Principles and Applications. Artech House, 2005.
26. T. Takasu and A. Yasuda, "Development of the low-cost RTK-GPS receiver with an open source program package RTKLIB," in Proc. of The International Symposium on GPS/GNSS, 2009.